[CANCER RESEARCH 58, 4832–4839, November 1, 1998]

Suppression of Tumor Promoter-induced Oxidative Stress and Inflammatory Responses in Mouse Skin by a Superoxide Generation Inhibitor 1′-Acetoxychavicol Acetate[1]

Yoshimasa Nakamura, Akira Murakami, Yoshimi Ohto, Koji Torikai, Takuji Tanaka, and Hajime Ohigashi[2]

Division of Applied Life Sciences, Graduate School of Agriculture, Kyoto University, Kyoto 606-8502 [Y. N., Y. O., K. T., H. O.]; Department of Biotechnological Science, Faculty of Biology-Oriented Science and Technology, Kinki University, Wakayama 649-6493 [A. M.]; and The First Department of Pathology, Kanazawa Medical University, Ishikawa 920-0293 [T. T.], Japan

ABSTRACT

Double applications of phorbol esters trigger excessive reactive oxygen species (ROS) production in mouse skin. Previously reported data suggest that the two applications induce distinguishable biochemical events, namely, priming and activation. The former is characterized as a recruitment of inflammatory cells, such as neutrophils, by chemotactic factors to inflammatory regions and edema formation. The latter is responsible for ROS generation. Thus, inhibitory effects of 1′-acetoxychavicol acetate (ACA), previously reported to be a superoxide generation inhibitor *in vitro*, on 12-*O*-tetradecanoylphorbol-13-acetate (TPA)-induced oxidative stress and inflammatory responses in mouse skin model were examined using a double application of ACA. We demonstrated that two pretreatments and pretreatment with ACA (810 nmol) in the activation phase suppressed double TPA application-induced H_2O_2 formation in mouse skin. ACA exhibited no inhibitory effects on edema formation and the enhancement of myeloperoxidase activity during the first TPA treatment, whereas the anti-inflammatory agent genistein administered at the same dose inhibited both biomarkers. No inhibitory potential of ACA for TPA-induced H_2O_2 formation in the priming phase was confirmed. On the other hand, in the *in vitro* study, ACA inhibited ROS generation in differentiated HL-60 cells more strongly than did 1′-hydroxychavicol, which showed no inhibition by pretreatment in the activation phase. In addition, allopurinol did not inhibit double TPA application-induced H_2O_2 formation in mouse skin. These findings suggest that the NADPH oxidase system of neutrophils rather than the epithelial xanthine oxidase system is dominant for the O_2^--generating potential in double TPA-treated mouse skin. ACA significantly inhibited mouse epidermis thiobarbituric acid-reacting substance formation, known as an overall oxidative damage biomarker. Moreover, histological studies demonstrated that ACA inhibited double TPA treatment-induced morphological changes reflecting inflammatory response, such as edema formation, leukocyte infiltration, hyperplasia, and cell proliferation. Furthermore, pretreatment with ACA but not 1′-hydroxychavicol in the activation phase inhibits its double TPA application-induced increases in both number of leukocytes and proliferating cell nuclear antigen index. These results suggested that ROS from leukocytes including O_2^- plays an important role for continuous and excessive production of chemotactic factors, leading to chronic inflammation and hyperplasia, which are inhibitable by ACA. Thus, we concluded that O_2^- generation inhibitors are agents that effectively inhibit oxidative stress and inflammatory responses in mouse skin.

INTRODUCTION

ROS[3] induce membrane damage, DNA base oxidation, DNA strand breaks, chromosomal aberrations, and protein alterations, most of which would be involved in the carcinogenesis process (1). Mounting evidence indicating some roles of oxidative stress in mechanisms of tumor promotion is currently widely accepted. For instance, organic peroxides and free radical generators have tumor-promoting activities in mouse skin, and inversely, antioxidants and free radical scavengers inhibit the biochemical and biological effects of tumor promoters and tumorigenesis (2). Tumor promoters such as TPA enhance the generation of ROS and decline the ROS detoxification enzymes in both epidermal and inflammatory cells. In the mouse skin model, TPA triggers ROS accumulation through the activation of the XA/XOD system or the stimulation of PMNs (2) and the inhibition of catalase or glutathione peroxidase (3). ROS are also generated enzymatically during the arachidonate metabolism. Kensler *et al.* (4) proposed a requirement of a two-dose application of TPA for massive ROS generation and the hypothesis that the first treatment of mouse skin with TPA application causes a chemotactic action (priming), *i.e.*, recruitment of neutrophils that are responsible for ROS generation with the second TPA treatment (activation; Ref. 5). ROS production by double or multiple TPA treatments is closely associated with the metabolic activation of proximate carcinogens (4–6) and the increased levels of oxidized DNA bases (7–9).

In our previous studies on the characterization of new types of chemopreventive agents through the scrutiny of diverse edible plants in southeast Asia (10–18), ACA (Fig. 1), isolated from the rhizomes of a Zingiberaceae plant *Languas galanga*, has attracted our attention as a potent inhibitor of tumor promoter-induced EBV activation (11). ACA has lately been found to suppress TPA-induced mouse skin tumor promotion (13), 4-nitroquinoline 1-oxide-induced rat tongue carcinogenesis (15), azoxymethane-induced rat colonic aberrant crypt foci formation (16), and tumorigenesis (17). ACA is known to be an inhibitor of XOD (19), which catalyzes the hydroxylation of many purine substances and generates superoxide (O_2^-), and this was confirmed in a recent study of ours as well (13). It should be noted that ACA potently inhibits TPA-induced O_2^- generation in differentiated HL-60 cells (13), whereas ACA is a much weaker antioxidant than α-tocopherol in the linoleate autooxidation system and has no O_2^- scavenging potential (13). Taken together, ACA is recognized to be a superoxide generation inhibitor but is not as radical a scavenger as are phenolic antioxidants. This is supported by the lack of phenolic hydroxyl groups in the chemical structure.

This study was undertaken to address whether ACA suppresses TPA-induced oxidative stress in mouse skin using the double-appli-

Received 6/8/98; accepted 9/2/98.

The costs of publication of this article were defrayed in part by the payment of page charges. This article must therefore be hereby marked *advertisement* in accordance with 18 U.S.C. Section 1734 solely to indicate this fact.

[1] Supported by grants-in-aid for Scientific Research on Priority Areas—Cancer—(to H. O.), Scientific Research Grant 10671782 (to T. T.), JSPS Research Fellow Grant (to Y. N.), and Encouragement of Young Scientists Grant 09760118 (to A. M.) from the Ministry of Education, Science, Sports, and Culture of Japan.

[2] To whom requests for reprints should be addressed, at Division of Applied Sciences, Graduate School of Agriculture, Kyoto University, Kyoto 606-8502, Japan. Phone: 81-75-753-6281; Fax: 81-75-753-6284; E-mail: ohigashi@kais.kyoto-u.ac.jp.

[3] The abbreviations used are: ROS, reactive oxygen species; TPA, 12-*O*-tetradecanoylphorbol-13-acetate; XA, xanthine; XOD, xanthine oxidase; PMN, polymorphonuclear leukocyte; ACA, 1′-acetoxychavicol acetate; DCFH-DA, 2′,7′-dichlorofluorescin diacetate; HC, 1′-hydroxychavicol; HRPO, horseradish peroxidase; IE, inhibitory effect; MPO, myeloperoxidase; DCF, 2′,7′-dichlorofluorescein; PPR, peroxidase positive rate; TBARS, thiobarbituric acid-reacting substance; PCNA, proliferating cell nuclear antigen.

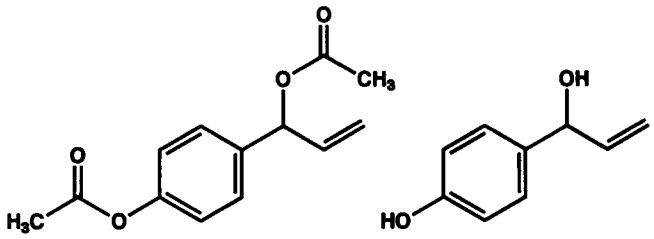

Fig. 1. Chemical structures of ACA (*left*) and HC (*right*).

cation model. Specific inhibition by ACA of the activation phase in H_2O_2 production induced by double TPA treatments is clarified. Further histological study clearly demonstrates the strong inhibition of inflammatory responses in mouse skin through ROS generation inhibition by ACA.

MATERIALS AND METHODS

Chemicals and Cells. TPA was obtained from Research Biochemicals International (Natick, MA). RPMI 1640 and fetal bovine serum were purchased from Life Technologies, Inc. (Rockville, MD). DCFH-DA was obtained from Molecular Probes, Inc. (Leiden, the Netherlands). Cytochrome *c* was obtained from Sigma Chemical Co. (St. Louis, MO). An authentic malondialdehyde (1,1,3,3-tetramethoxypropane) was purchased from OXIS International Inc. (Portland, OR). All other chemicals were purchased from Wako Pure Chemical Industries (Osaka, Japan). ACA and HC were synthesized as reported previously (11). HL-60 cells were obtained from the Health Science Research Resources Bank (Osaka, Japan; Ref. 20).

Treatment of Animals. Female ICR mice (7 weeks old) were obtained from Japan SLC (Shizuoka, Japan). Mice used in each experiment were supplied with fresh tap water *ad libitum* and rodent pellets (MF; Oriental Yeast Co., Kyoto, Japan), changed twice a week. Animals were maintained in a room controlled at 24 ± 2°C with a relative humidity of 60 ± 5% and a 12-h light/dark cycle (light from 6:00 a.m. to 6:00 p.m.). The back of each mouse was shaved with surgical clippers 2 days before each experiment. All test compounds (100 μl in acetone) were topically applied to the shaved area of dorsal skin 30 min before application of a TPA solution (8.1 nmol/100 μl in acetone). In the double-treatment protocol, the same doses of TPA and test compounds or acetone were applied twice with an interval of 24 h, as shown in Fig. 2.

Determination of H_2O_2 in Mouse Skin. Mice treated with a double-treatment protocol were sacrificed 1 h after the second TPA treatment. Their skins were removed and then immersed in a 55°C water bath for 30 s, and the subcutis was scraped off. Skin (epidermis and dermis) punches were obtained with an 8-mm-diameter cork borer and weighed on an analytical balance. The skin punches were minced in 3 ml of 50 mM phosphate buffer (pH 7.4) containing 5 mM sodium azide and then homogenized twice at 4°C for 30 s each. The homogenate was centrifuged at 10,000 × *g* for 20 min at 4°C. The H_2O_2 content was determined by the phenol red-HRPO method (7, 21). To each 1.5-ml cuvette, 0.5 ml of the homogenate supernatant and 0.5 ml of the phenol red (200 μg/ml)-HRPO (100 μg/ml) solution were added and incubated at 25°C for 10 min. At the end of the incubation, 100 μl of 1 M NaOH were added to terminate the reaction, and then the visible absorbance was determined spectrophotometrically at 610 nm. The final results were expressed as equivalents of nanomoles of H_2O_2 per skin punch, on the basis of a standard curve of HRPO-mediated oxidation of phenol red by H_2O_2.

Anti-Inflammation Test in Mouse Skin. IE on single TPA application-induced inflammation was determined by two biomarkers, edema formation, and MPO activity by the method of Wei and Frenkel (7), with slight modifications. Mice were sacrificed by cervical dislocation 18 h after a single application of TPA. The mouse skin punches were obtained with an 8-mm-diameter cork borer and weighed on an analytical balance. The IEs were expressed by the relative ratio of differences in the weight of a treated punch and that of a control punch as follows: IE (%) = [(TPA alone) − (test compound plus TPA)]/[(TPA) − (vehicle)] × 100. Statistical analysis was done by the Student's *t* test. For the determination of MPO activity, the skin punches were minced in 3 ml of 0.5% hexadecyltrimethyl ammonium bromide in 50 mM potassium phosphate buffer (pH 6.0) and homogenized twice at 4°C for 10 s. Samples were centrifuged at 10,000 × *g* for 20 min at 4°C. To each 2-ml cuvette, 0.65 ml of 25 mM 4-aminoantipyrine-2% phenol solution and 0.75 ml of 2 mM H_2O_2 were added to equilibrate for 5 min. After the basal rate was established, a 100-μl sample supernatant was added to the cuvette and quickly mixed. Increases in absorption at 510 nm for 1 min at 0.1-min intervals were recorded. The MPO activity was calculated from the linear portion of the curve and expressed as units of MPO per skin punch. One unit of MPO activity is defined as the activity that degrades 1 μmol of H_2O_2 per min at 25°C.

Inhibitory Tests of TPA-induced O_2^- Generation and Intracellular Peroxide Formation in Differentiated HL-60 Cells. Inhibitory tests of TPA-induced O_2^- generation in DMSO-differentiated HL-60 cells were performed as reported previously (22, 23). Briefly, to determine the IE of O_2^- generation, a test compound dissolved in 5 μl of DMSO was added to DMSO-induced differentiated HL-60 cell suspension and incubated at 37°C for 15 min. The cells were washed with PBS twice for removal of extracellular test compound to eliminate the O_2^- scavenging effect. TPA (100 nM) and cytochrome *c* solution (1 μg/ml) were added to the reaction mixture, which was incubated for another 15 min. The reaction was terminated by placing it on ice. After centrifugation at 250 × *g*, the visible absorption at 550 nm was measured. The IE was expressed by the relative decreasing ratio of absorbance of a test compound to that of a control.

Intracellular peroxides were detected by DCFH-DA as an intracellular fluorescence probe (23, 24). A flow cytometer (CytoACE 150; JASCO, Tokyo, Japan) was used to detect DCF formed by the reaction of DCFH with intracellular peroxides. The TPA-treated cells showing fluorescence levels equal to the mean plus three SDs of that of the control cells or higher were regarded as "peroxide positive," and their rates were expressed as a "PPR." Experimentation was repeated twice with similar results. The data were expressed by a representative histogram.

Determination of TBARS in Mouse Epidermis. Mice treated with a double-treatment protocol were sacrificed 1 h after the second TPA treatment. Skin samples from treated areas were excised and immediately dipped into ice-cold PBS. After subcutis were scrapped off, the skin was cut into small pieces and floated, epidermis side down, in a culture dish with a 2.5% trypsin solution at 37°C for 45 min. The epidermis was then scrapped off and placed

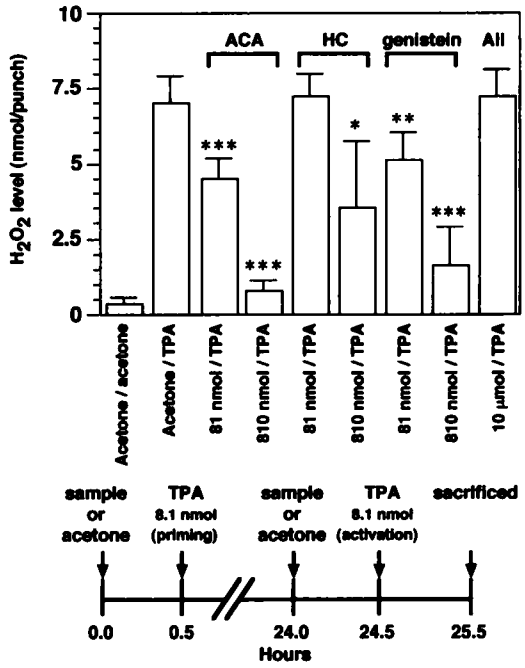

Fig. 2. IEs of ACA, HC, genistein, and allopurinol on H_2O_2 formation in mouse skin. ICR mice (5 mice in each group) were treated by a double TPA treatment protocol. Mouse skin was treated with test compound (81 and 810 nmol) or allopurinol (*All*, 10 μmol) or acetone 30 min prior to each TPA treatment. The mice were sacrificed 1 h after the second TPA application, and their skins were removed. Significance, determined by the Student's *t* test, is expressed as follows: *, $P < 0.05$; **, $P < 0.01$; ***, $P < 0.001$, all *versus* TPA.

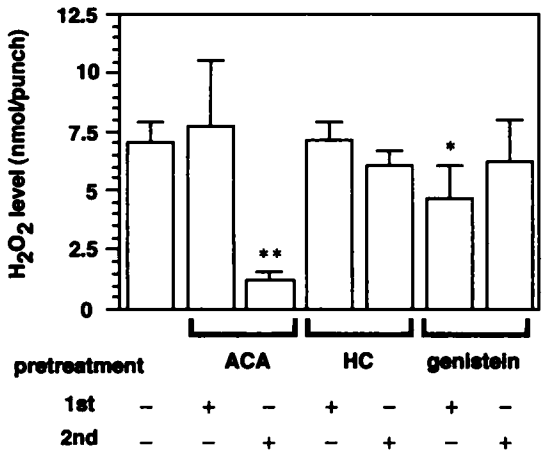

Fig. 3. IEs of ACA, HC, and genistein applied in the priming or activation phase on H_2O_2 formation in mouse skin. Mice (five mice in each group) were treated with ACA, HC, or genistein (810 nmol) or acetone 30 min before either first or second TPA treatment. The mice were sacrificed 1 h after the second TPA application. Significance, determined by the Student's t test, is expressed as follows: *, $P < 0.05$; **, $P < 0.001$, both *versus* TPA.

into a cuvette with 450 μl of 50 mM phosphate buffer (pH 7.4). Fifty μl of 50% trichloroacetic acid solution was added and sonicated for 10 min. After five freeze-thaw cycles, the sample was centrifuged for 10 min at 10,000 × g. The TBARS level of mouse epidermis was determined by a previously reported method (14). The final results were expressed as equivalents of nanomoles of malondialdehyde per cm^2, on the basis of a standard line of TBARS formation using an authentic malondialdehyde.

Histological Examination. Mice treated with a double-treatment protocol were sacrificed 1 h after the second TPA treatment. Excised skin was fixed in 10% buffered formalin and then embedded in paraffin. Skin samples were cut at 3 μm and mounted on silanized slides. Slides were dewaxed in xylene, dehydrated through an ethanol series, and finally, after staining, dehydrated and mounted in Permount medium. Histological alteration was evaluated by H&E staining. For each section of skin, the thickness of the epidermis from the basal layer to the stratum corneum was measured at five equidistant interfollicular sites using an image analysis system Leica Q500IW-EX (Leica Co., Ltd., Tokyo, Japan) with a microscope Leica DMRE HC (Leica Co., Ltd.). The numbers of infiltrating leukocytes were counted at five different areas of each section using this image analysis system.

PCNA Immunohistochemistry. Skin sections were treated with 1.2% H_2O_2 in absolute methanol for 30 min and stained by the indirect abidin-biotin-HRPO method (ABC standard; Vector Laboratories, Burlingame, CA). Color development with diaminobenzidine (Vector Laboratories) was monitored by appearance of the normal PCNA brown staining in normal epidermis. The primary antibody to PCNA (PC10; Boehringer Mannheim, Mannheim, Germany) was applied at a 1:300 concentration overnight at 4°C. Negative controls without primary antibody were included. Sections were counterstained with hematoxylin for quantification of stained and nonstained cells. The PCNA index was counted at six different areas of each section using the image analysis system and expressed as the number of positive squamous cells divided by the total number of squamous cells times 100.

RESULTS

IEs of ACA, HC, Genistein, and Allopurinol on TPA-induced H_2O_2 Production in Mouse Skin. HC is regarded as an appropriate analogue for *in vivo* antioxidative studies because it is negative in tumor promoter-induced EBV activation (11). As shown in Fig. 2, double applications of 8.1 nmol of TPA at 24-h intervals increased the level of H_2O_2 by ~20-fold (7.01 ± 0.87 *versus* 0.36 ± 0.25 nmol/skin punch, $P < 0.001$) over that in the control mice treated twice with acetone instead of TPA. The requirement of second TPA treatment for ROS production was pointed out by Ji and Marnett (5) and was also confirmed in these experiments, in which a single-dose application of TPA did not significantly enhance H_2O_2 production 1–24 h after treatment (values 1 h and 18 h after application were 0.30 ± 0.18 nmol/skin punch and 0.50 ± 0.28 nmol/skin punch, respectively). Pretreatment of ACA (810 nmol) before each TPA treatment almost completely inhibited H_2O_2 formation (0.79 ± 0.38 nmol/skin punch, IE = 89%). Genistein at the same dose also significantly reduced H_2O_2 formation (1.63 ± 1.27 nmol/skin punch, IE; 77%). Both compounds reduced the H_2O_2 level in a dose-dependent manner. On the other hand, HC at 810 nmol weakly inhibited H_2O_2 formation by 49% and showed no IE at 81 nmol. Allopurinol, a well-known XOD inhibitor, even at a dose of 10 μmol, did not reduce the H_2O_2 level. ACA and HC have no effect on the level of externally added H_2O_2 *in vitro* (data not shown), whereas genistein was reported to be a H_2O_2 scavenger (21). The possibility of up-regulation of glutathione levels that decompose H_2O_2 may be ruled out in this mechanism because ACA showed no influence on total glutathione levels and significantly decreased oxidized glutathione levels in double TPA applications (data not shown).

IEs of ACA, HC, and Genistein Applied in the Priming or Activation Phase on TPA-induced H_2O_2 Generation in Mouse Skin. To distinguish whether ACA, HC, and genistein inhibit the priming or activation phase in a double TPA application model, each test compound was coadministered with either the first (priming) or second (activation) dose of TPA. Fig. 3 shows the IEs of ACA, HC, and genistein applied prior to either the first or second TPA treatment on H_2O_2 generation in mouse skin. A dramatic decrease in the H_2O_2 level was observed in the mice to which ACA was coadministered in the activation phase (1.24 ± 0.29 nmol/skin punch, IE; 87%). On the contrary, ACA applied in the priming phase exhibited no inhibition of H_2O_2 generation. HC showed no significant decrease in H_2O_2 level in the priming phase and only weak inhibition in the activation phase. Genistein reduced the H_2O_2 level in both phases, and inhibition was remarkable in the priming phase but not in the activation phase (4.68 ± 1.43 *versus* 6.28 ± 1.43 nmol/skin punch).

IEs of ACA, HC, and Genistein on Single TPA Application-induced Mouse Skin Inflammation. The effects of ACA, HC, and Genistein on single application of TPA-induced inflammation, determined by skin edema formation and PMN infiltration, were examined. As shown in Table 1, single TPA application (8.1 nmol) resulted in an increase in edema formation (as measured by the weight of skin punch) by 3.2-fold (99.8 ± 5.8 *versus* 31.2 ± 6.1 mg/skin punch, $P < 0.001$) and in PMN infiltration (as measured by MPO activity) by 2.5-fold (6.99 ± 0.72 *versus* 2.80 ± 0.52 unit/skin punch, $P < 0.001$), as compared with the control. Pretreatment with neither ACA nor HC at a 100-fold molar dose to TPA (810 nmol) reduced skin edema formation and PMN infiltration. Genistein at 810 nmol significantly inhibited both biomarkers by 36 and 47%, respectively.

Table 1 *Inhibitory activities of ACA, HC, and genistein (810 nmol) against inflammation induced by single dose of TPA in mouse skin*

ICR mice (5 mice in each group) were treated as described in "Materials and Methods." The mice were sacrificed 18 h after TPA treatment (8.1 nmol), and skin punches were obtained for determination of edema formation and MPO activity.

Treatment	Edema (mg/punch)		MPO (units/punch)	
	Mean ± SD[a]	IE (%)	Mean ± SD[a]	IE (%)
Acetone/acetone	31.2 ± 6.1		2.8 ± 0.5	
Acetone/TPA	99.8 ± 5.8[b]		7.0 ± 0.7[b]	
ACA/TPA	97.7 ± 6.8[b]	3	6.2 ± 1.4[b]	19
HC/TPA	99.2 ± 5.2[b]	0.9	7.9 ± 0.8[b]	−21
Genistein/TPA	75.5 ± 2.6[b,c]	36	5.0 ± 0.6[b,c]	47

[a] Significance was determined by the Student's t test.
[b] $P < 0.001$ *versus* acetone/acetone control.
[c] $P < 0.001$ *versus* acetone/TPA.

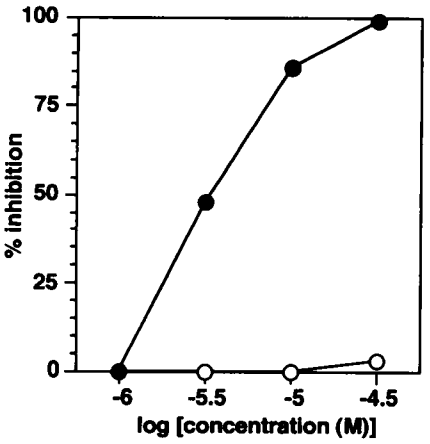

Fig. 4. IEs of ACA and HC on O_2^- generation in differentiated HL-60 cells. HL-60 cells were preincubated with 1.25% DMSO at 37°C for 6 days, which differentiated them into granulocyte-like cells. ACA (●) or HC (○) solution was added to the cell suspension, and the mixture was incubated at 37°C for 15 min, followed by washing with PBS twice. Ninety s after stimulation with TPA (100 nM), cytochrome *c* solution was added to the reaction mixture. After incubation for another 15 min followed by centrifugation, visible absorption at 550 nm was measured. The maximal SD for each experiment was 5% (n = 2).

***In Vitro* IEs of ACA and HC on TPA-induced O_2^- Generation and Intracellular Peroxide Formation.** Because ACA but not HC, applied in the activation phase when ROS are generated by inflammatory cells in mouse skin, showed a significant inhibition against H_2O_2 generation, we examined IEs of ACA and HC on ROS generation in leukocytes. The differentiated HL-60 cell system was chosen as a model of the NADPH oxidase system. IE of ACA on O_2^- generation in differentiated HL-60 cells was indirectly confirmed in the previous study (13). The possibility of O_2^- scavenging by ACA was raised because ACA coexisted with O_2^- in the previous experimental condition. No O_2^- scavenging potential of ACA was confirmed in the different system (XA/XOD system). To confirm directly whether or not ACA inhibits O_2^- generation, TPA stimulation was carried out after removing ACA from the reaction mixture by washing with PBS. As shown in Fig. 4, ACA strongly inhibited O_2^- generation (IC_{50} = 4.5 μM) in the same concentration-dependent manner, as reported previously (IC_{50} = 4.3 μM; Ref. 13), whereas HC, even at a concentration of 80 μM, was inactive in O_2^- generation assays. HC did not scavenge O_2^- up to 100 μM in the XA/XOD system (data not shown). Inhibitory activities against the formation of peroxides, including hydrogen peroxide (H_2O_2) and lipid hydroperoxides, in differentiated HL-60 cells were determined by using DCFH-DA as an intracellular fluorescence probe. Most of the cells were estimated to produce peroxides (PPR = 97%) with TPA stimulation alone. ACA at a concentration of 10 μM significantly inhibited peroxide formation by 81%. PPRs and IEs of test compounds are shown in Fig. 5. HC was inactive up to a concentration of 100 μM.

IE of ACA on TPA-induced TBARS Formation in Mouse Epidermis. Because topically applied ACA afforded significant inhibition against double TPA application-induced H_2O_2 generation, we assessed whether such ACA treatment reduces double TPA application-induced TBARS formation, a well-known biomarker of overall oxidative damage to cellular constituents such as membrane lipids. The quantitative data for the level of TBARS formation in mouse epidermis homogenate detected in each group are shown in Fig. 6. The increased level in TBARS caused by the single TPA application was highly significant to that of the control (0.52 ± 0.05 *versus* 0.36 ± 0.25 nmol/cm^2, $P < 0.01$). The net increase in TBARS level (control values subtracted) after the second application of TPA (0.40 nmol/cm^2) was 2.5-fold higher than that caused by a single TPA treatment (0.16 nmol/cm^2). Pretreatment of ACA (810 nmol) before each TPA treatment inhibited the increase of TBARS level by the second application of TPA (0.41 ± 0.14 nmol/cm^2, $P < 0.01$ *versus* double TPA). These data indicate that ACA significantly inhibits TBARS formation (Fig. 6).

Effects of ACA on Morphological Alteration in Mouse Skin Treated with Double TPA Applications. The results that double TPA treatment caused a dramatic increase in H_2O_2 levels led us to select this protocol for histological observation to determine whether TPA application(s) enhance edema formation, leukocyte infiltration, and hyperplasia in the skin. A single application of TPA caused morphological alteration of inflammatory response (Table 2 and Fig. 7*B*), as compared with the control group (Fig. 7*A*), which was well correlated to the results of skin edema formation and MPO activity (Table 1). Mouse skin treated with TPA twice with a 24-h interval displayed severe epidermal hyperplasia (Fig. 7*C*) and resulted in an ~2-fold increment in leukocyte infiltration, as compared with that treated with a single TPA application, as shown in Table 2 (169 ± 43 *versus* 294 ± 27/mm^2). Also, double TPA treatment increased the

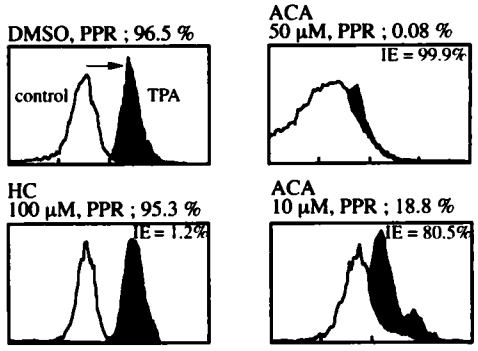

Fig. 5. DCF fluorescence distribution in DMSO-differentiated HL-60 cells. Cells were preincubated with 50 μM DCFH-DA at 37°C for 15 min. After being treated with DMSO (positive control) at 37°C for 15 min, the cells were treated with ethanol (unstimulated control, *open cytogram*) or 100 nM TPA (*closed cytogram*). As for inhibition of ACA and HC, cells were preincubated with 50 μM DCFH-DA at 37°C for 15 min. After being treated with the test compound at 37°C for 15 min, the cells were treated with ethanol (*left*) or 100 nM TPA (*right*). The DCF fluorescence was monitored on a flowcytometer (CytoACE 150) with excitation and emission wavelengths at 488 nm and 510 nm, respectively. *X axis*, relative fluorescence intensity; *Y axis*, cell count.

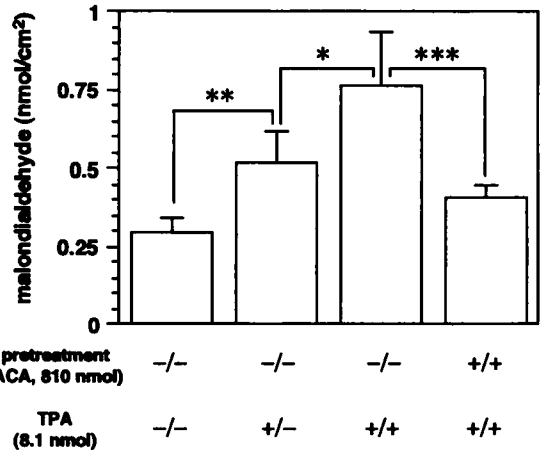

Fig. 6. IEs of ACA on the TBARS formation in mouse epidermis. ICR mice (five mice in each group) were treated by the double treatment protocol as described in "Materials and Methods." Mouse skins were treated with ACA (810 nmol) or acetone 30 min prior to each TPA treatment. The mice were sacrificed 1 h after the second TPA application, and the epidermis was removed for TBARS assays. The mice with single TPA were treated with TPA only in the priming phase. Significance, determined by the Student's *t* test, is expressed as follows: *, double TPA *versus* single TPA, $P < 0.05$; **, single TPA *versus* acetone control, $P < 0.01$; ***, double ACA/TPA *versus* double TPA, $P < 0.01$.

Table 2 *Double TPA treatment-induced morphological changes in mouse skin*

Treatment[a]		Epidermal thickness (μm)[b]	No. of epidermal layers[c]	No. of leukocytes in the cutis[d]	PCNA-stained cell nuclei index
Pretreatment	TPA (1st/2nd)				
Acetone	(−/−)	23.4 ± 2.9	2 (1–2)	8 ± 3	51.2 ± 7.6
Acetone	(+/−)	32.1 ± 4.0[e]	4 (3–4)	169 ± 43[e]	79.4 ± 9.8[e]
Acetone	(+/+)	35.4 ± 4.5[e]	4 (2–5)	294 ± 27[e,f]	84.8 ± 7.3[e]
ACA × 2	(+/+)	38.8 ± 3.7[e]	3 (2–4)	98 ± 44[e,g]	57.7 ± 9.2[e,g]

[a] Mice were treated as described in "Materials and Methods." The mice were sacrificed 1 h after the second TPA treatment (8.1 nmol), and skin punches were obtained for determination of the morphological changes.

[b] Hyperplastic response of the skin determined in a section (3 μm) of skin. Values are means ± SD of 15 values taken from three individual mice.

[c] Majority (range) of 15 values, counted in the various regions.

[d] Mean ± SD of 15 values, counted in various regions of the cutis (dermis and subcutis) in an area of 1 mm^2 under a microscope.

[e] Significant *versus* acetone and TPA (−/−) (Student's *t* test); $P < 0.05$.

[f] Significant *versus* acetone and TPA (+/−) (Student's *t* test); $P < 0.05$.

[g] Significant *versus* acetone and TPA (+/+) (Student's *t* test); $P < 0.05$.

number of mitosis in epidermal squamous cells when compared with single TPA application (Fig. 7, *B* and *C*). On the other hand, pretreatment of ACA (810 nmol) before each TPA application diminished TPA-induced hyperplasia, mitosis (Fig. 7, *C* and *D*) and leukocyte infiltration (Table 2).

PCNA-stained Cell Nuclei Index. PCNA immunohistochemistry revealed PCNA-stained nuclei in many epidermal keratinocytes, only at the basal and first suprabasal layer in mice treated with acetone alone (PCNA index = 51.2 ± 7.6; Table 2 and Fig. 8). A single application significantly increased the PCNA index (79.4 ± 9.8, $P < 0.02$) in the epidermis when compared with that of control mice (treated with acetone alone). Double application of TPA slightly enhanced the PCNA index (84.8 ± 7.3) when compared with a single application of TPA. However, the PCNA index (57.7 ± 9.2) in mice given double application of TPA and ACA was almost equal to that of control mice, and the value was significantly lower than that of mice treated twice with TPA ($P < 0.02$). Although a high proportion of epithelial cell nuclei in hair follicles and glandular appendages was also stained, no significant differences in this pattern were observed between different treatment groups (Fig. 8).

IEs of ACA Applied in the Priming or Activation Phase on the Number of Leukocytes in the Dermis and the PCNA Index. Because topically applied ACA afforded a significant inhibition against double TPA application-induced leukocyte infiltration, we counted the number of leukocytes infiltrated into the dermis and measured PCNA indexes in the double TPA treatment protocol. As shown in Fig. 9, significant decreases in numbers of leukocytes and the PCNA index were observed in the mice to which ACA was coadministered in the activation phase (IE of leukocytes = 45%; IE of PCNA = 33%). In contrast, ACA applied in the priming phase and HC applied in both phases exhibited no inhibition.

DISCUSSION

Double applications of phorbol esters trigger ROS production in mouse skin (4, 6). The available data suggest that each application induces two distinguishable biochemical events, namely, priming and activation (5). The former is characterized as recruitment of inflammatory cells such as neutrophils by chemotactic factors to inflamma-

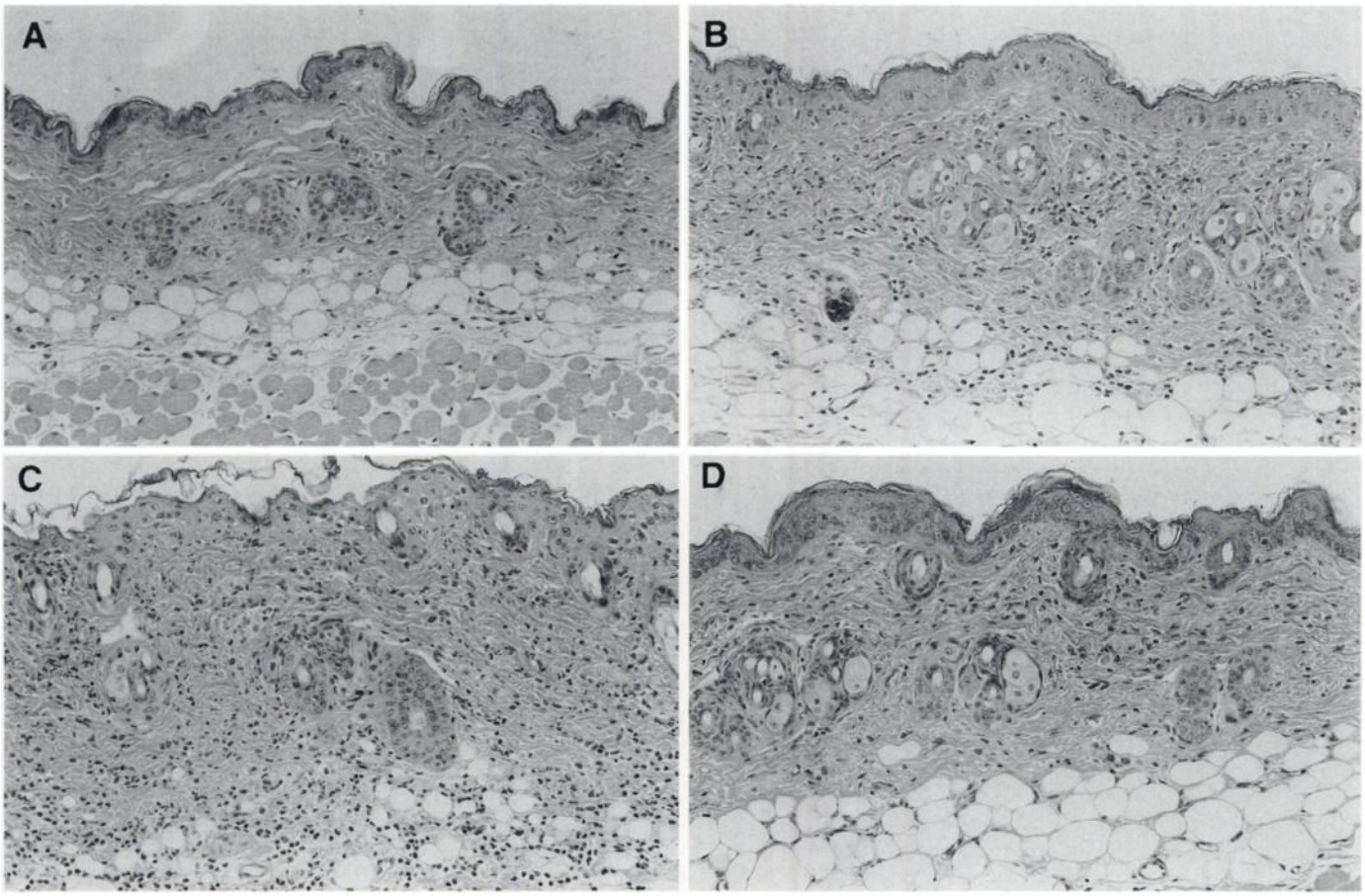

Fig. 7. Effect of ACA on TPA-induced mouse skin morphological changes. The protocol for animal treatment was as described in "Materials and Methods." Treatment was as follows: *A*, acetone; *B*, single dose of TPA in the priming phase; *C*, double dose of TPA; *D*, double dose of ACA and TPA. ×20.

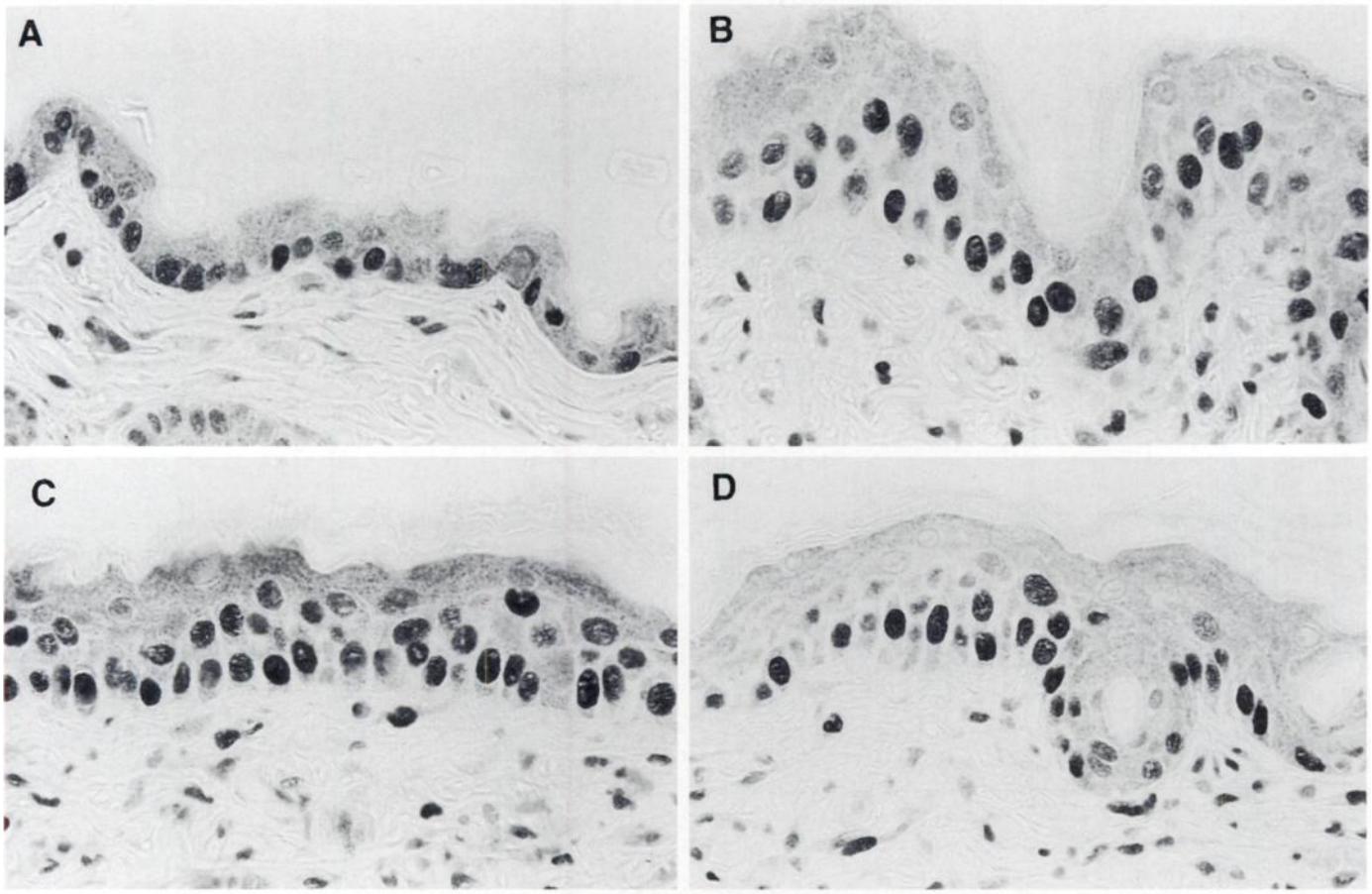

Fig. 8. Immunohistochemical demonstration of nuclear expression of PCNA. The protocol for animal treatment was as described in "Materials and Methods." Treatment was as follows: *A*, acetone; *B*, single dose of TPA in the priming phase; *C*, double dose of TPA; *D*, double dose of ACA and TPA. ×40.

tory regions and edema formation. The latter is the process of activation of neutrophils or other oxidant-producing cells, including keratinocytes, in which the second TPA application of phorbol esters induces oxidative stress. In this study, single application of TPA (8.1 nmol) significantly increased the weight of a skin punch as well as MPO activity, a biomarker for infiltration of the inflammatory cells into the target tissue (Table 1). Double treatments of ICR mice with TPA (8.1 nmol) dramatically increased the formation of H_2O_2 in the skin (Fig. 2) as previously reported using outbred species of mice such as SENCAR or CD-1 (7, 21). Importantly, the TPA dose used in this experiment is in the tumor promotion range (1–10 nmol).

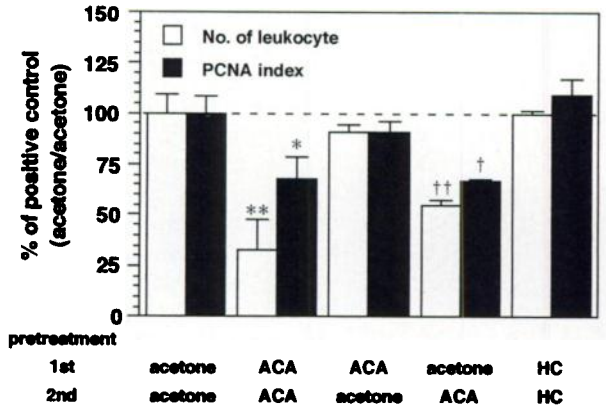

Fig. 9. IEs of ACA applied in the priming or activation phase and HC on double TPA application-induced increment of number of leukocyte in the dermis and PCNA-stained cell nuclei index. Significance, determined by the Student's *t* test or Welch's *t* test ($n = 3$), is expressed as follows: *, $P < 0.05$; **, $P < 0.001$, both *versus* acetone control; and †, $P < 0.01$; ††, $P < 0.001$, both *versus* acetone control.

These results provide clear evidence for the suppression of tumor promoter-induced H_2O_2 formation in mouse skin by ACA. It is noteworthy that ACA exhibited no IEs on edema formation and the enhancement of MPO activity in the first TPA treatment, whereas a radical scavenger, genistein, administered at the same dose (810 nmol) significantly suppressed these inflammatory biomarkers (Table 1). No inhibitory potential of ACA for the TPA-induced priming phase was clearly confirmed by the experiment in which ACA was coadministered only with the first dose of TPA (Fig. 3). It is likely that induction of lipoxygenase, which metabolizes arachidonic acid to hydroperoxy fatty acids, precursors of chemotactic leukotrienes, represents an earlier stage in the priming phase (5). Indeed, anti-inflammatory curcumin, reported to be an arachidonate metabolism inhibitor, suppressed the priming effect of double TPA application-induced H_2O_2 generation (23). Conversely, ACA showed no IEs on TPA-induced arachidonate release or prostaglandin E_2 synthesis in HeLa cells.[4] Taken together, the inhibition of some biological events in the priming phase by ACA can be ruled out from the critical mechanisms of H_2O_2 generation inhibition *in vivo*.

Coadministration of ACA with only the second TPA treatment successfully inhibited H_2O_2 formation, whereas HC and genistein in the same treatment failed to do so (Fig. 3). A well-known XOD inhibitor, allopurinol, also showed no IE on double TPA treatment-induced H_2O_2 generation. These findings appeared to be consistent

[4] A. Murakami, Y. Nakamura, and H. Ohigashi, unpublished observation.

with a mechanism in which the NADPH oxidase system of neutrophils rather than the epithelial XOD system is implicated in the O_2^--generating system in double TPA-treated mouse skin. Single-dose TPA-induced enhancement of XOD activity was reported (25), but in this study, single-dose TPA did not significantly enhance H_2O_2 formation, suggesting the critical role of NADPH oxidase system in double TPA application-induced oxidative stress. Single TPA application enhances oxidized DNA base formation to a much lesser degree than do double applications of TPA (9), also supporting this suggestion.

In vitro, ACA exhibited potent inhibition of O_2^- generation (IC_{50} = 4.5 μM; Fig. 4). In contrast, the inhibitory activities of HC (>100 μM) and genistein (102 μM; Ref. 13) were much weaker than that of ACA. Thus, there is a positive correlation between inhibition of the activation phase *in vivo* and suppression of leukocyte activation *in vitro*. It is interesting to note that HC, having two hydroxyl groups that generally play essential roles for radical scavenging of phenolic antioxidants, has weaker IEs on tumor promoter-induced ROS generation *in vivo* and *in vitro*, whereas it shows a much stronger antioxidative effect on the propagation of lipid peroxidation than does ACA.[5]

Takeuchi *et al.* (26) have indicated that extracellular O_2^- in HL-60 cells may be generated by plasma membrane-bound NADPH oxidase and diffuse into the cells through the anion channel, but intracellular H_2O_2 may be formed extracellularly from O_2^-, being diffused into the cells through membrane. Lundqvist *et al.* (27) also confirmed the origin of intracellular H_2O_2 by the observation that differentiated HL-60 cells, lacking specific granules in which all membrane components necessary for NADPH oxidase activity are present, showed a much lower intracellular chemiluminescence response than did the isolated neutrophils having specific granules. These findings also support the idea that ACA suppresses intracellular peroxide formation due to inhibition of plasma membrane-bound NADPH oxidase. The exact mechanism for the inhibition of NADPH oxidase activity by ACA remains to be clarified. It should be noted that staurosporine, a microbial alkaloid protein kinase C inhibitor without antioxidative activity, inhibits O_2^- production in neutrophils (28). It is interesting that ACA does not alter protein kinase C activity (29), suggesting the existence of novel pathway(s) for inhibition of the NADPH oxidase system. In any case, more extensive mechanistic studies on the inhibition of TPA-induced O_2^- generation by ACA are necessary.

These data indicate that ACA, a weak antioxidant in lipid peroxidation *in vitro* (13), significantly inhibits TBARS formation (Fig. 6), known as an overall oxidative damage biomarker, which was, at least in part, formed downstream of H_2O_2 generation in the presence of a metal ion as catalyst. TBARS formation *in vivo* is not considered to reflect a single particular phenomenon but is considered to indicate widespread oxidative damage, including lipid peroxidation, mitochondrial deenergization, and degradation of protein or sugar rather than DNA (30). Cell death and subsequent regenerative cell proliferation, which gives growth advantage to phenotypically altered populations, are accepted to play critical roles in some kinds of organ carcinogenesis in rodents (31). The IE of ACA on double TPA application-induced morphological changes in mouse skin, such as mitosis of epidermal cells or PCNA index (Table 2 and Figs. 7 and 8), suggested that suppression of cell proliferation is an important action mechanism of antitumor promotion.

Other possible mechanisms are considered. Wei and Frenkel (7–9) found the increased levels in oxidized DNA bases in mice with double TPA treatment and with multiple TPA treatment for 16 weeks. The positive correlation among the formation of H_2O_2, oxidized DNA bases, and first-stage tumor-promoting activity has been described (8, 9). Alternatively, hydroxyl radicals react with membrane lipids to form hydroperoxides which are then decomposed and converted to mutagenic, reactive carbonyl compounds, such as malondialdehyde. On the other hand, the oxidative metabolic activation of proximate carcinogens, independent of the cytochrome P-450 pathway, has been proven to be associated with multiple treatments on mice with a tumor promoter (4–6). It has been presumed that not only the stimulation of DNA synthesis but also remodeling of the epidermal metabolic pathway from the cytochrome P450-dependent pathway to an oxygen radical-dependent pathway increases the probability of mutation (5). MPO was also involved in the bioactivation of a procarcinogen in mouse skin and lung (4, 6, 31, 32). Thus, the suppressing effects of ACA against TPA-induced H_2O_2 generation suggested the possibility that ACA may inhibit these oxidative events, which are closely related to mutagenesis.

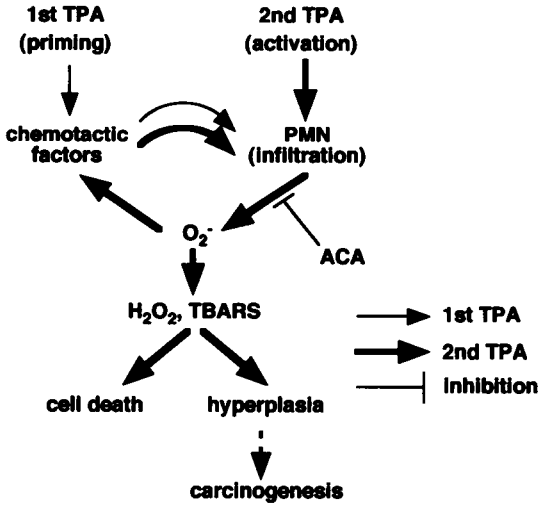

Fig. 10. Proposed action mechanism of ACA for suppression of inflammation in mouse skin.

Histological studies demonstrated very clearly that double TPA treatments enhance morphological changes, reflecting inflammatory response. A single application of TPA induces edema formation and leukocyte infiltration, similar to the result of biochemical detection (Tables 1 and 2). Surprisingly, a significant increase (1.7-fold) in leukocyte infiltration was observed 1 h after the second TPA application (Table 2 and Fig. 7). It should be noted that, although inhibiting neither the arachidonate metabolism nor single application-induced edema formation, ACA could reduce the increment in numbers of leukocytes in mouse cutis, but HC without O_2^- generation inhibition showed no suppression (Table 2 and Fig. 9). Kensler *et al.*, (6) presumed that the second TPA could additionally recruit leukocytes, which are phenotypically different from those recruited by a single TPA treatment. In this respect, it is important to note that O_2^- is known to participate in the formation of chemotactic factors and recruitment of PMNs (33). Thus, it is tempting to recognize that suppression of leukocyte infiltration by ACA, which was observed in the histological study, is attributable to the inhibition of the second dose of TPA-induced O_2^- generation by leukocytes. These data clearly demonstrated that pretreatment of ACA, only in the activation phase, successfully inhibits double TPA application-induced increment in both numbers of leukocyte and PCNA index (Figs. 8 and 9). This result strongly suggested that O_2^- from leukocytes plays an important role for continuous and excessive production of chemotactic factors, leading to chronic inflammation and hyperplasia (Fig. 10).

[5] Y. Nakamura, A. Murakami, and H. Ohigashi, unpublished observation.

The positive correlation between the formation of cytotoxic TBARS and increment in numbers of infiltrated leukocytes (Table 2 and Fig. 6) supported this suggestion.

In any case, we concluded that a O_2^- generation inhibitor ACA potently suppresses double TPA application-induced oxidative stress and inflammatory responses mainly *via* inhibition of ROS generation by leukocytes. In a rat oral carcinogenesis model, inflammatory cell infiltration is predominant in macrophage, which is related to immune function alteration, 5–6 months after oral carcinogenic 4-nitroquinoline 1-oxide treatment (34). It is well known that chronic inflammation of the colon is associated with an increased risk of colorectal cancer. Recently, neutrophil-mediated nitrosamine formation has been indicated to be a possible endogenous carcinogen, which may promote neoplasia (35). Interestingly, ACA exhibited chemopreventive effects on chemically induced carcinogenesis in rat colon and tongue, with which acute and/or chronic inflammation are considered to be closely associated. Suppressive effects of ACA on leukocyte-derived ROS formation may be, in part, involved in a common mechanism for the inhibition of inflammation-related carcinogenesis. Studies on the influences of ACA on immune function such as natural killer activity or the T cell-mediated immune system as well as investigation of ACA in a wide range of animal carcinogenesis models relating to inflammation are necessary.

ACKNOWLEDGMENTS

We thank Dr. M. A. Huffman for his critical reading and helpful comments on earlier versions of this manuscript.

REFERENCES

1. Cerutti, P. A. Proxidant states and tumor promotion. Science (Washington DC), *227:* 375–380, 1985.
2. Perchellet, J. P., Perchellet, E. M., Gali, H. U., and Gao, X. M. Oxidative stress and multistage skin carcinogenesis. *In:* H. Mukhtar (ed.), Skin Cancer: Mechanisms and Human Relevance, pp. 145–180. Boca Raton, FL: CRC Press, 1995.
3. Solanki, V., Rana, R. S., and Slaga, T. J. Diminution of mouse epidermal superoxide dismutase and catalase activities by tumor promoter. Carcinogenesis (Lond.), *2:* 1141–1146, 1981.
4. Kensler, T. W., Egner, P. A., Moore, K. G., Taffe, B. G., Twerdok, L. E., and Trush, M. A. Role of inflammatory cells in the metabolic activation of polycyclic aromatic hydrocarbons in mouse skin. Toxicol. Appl. Pharmacol., *90:* 337–346, 1987.
5. Ji, C., and Marnett, L. J. Oxygen radical-dependent epoxydation of (7*S*,8*S*)-dihydroxy-7,8-dihydrobenzo[a]pyrene in mouse skin *in vivo*. Stimulation by phorbol esters and inhibition by antiinflammatory steroids. J. Biol. Chem., *267:* 17842–17878, 1992.
6. Kensler, T. W., Egner, P. A., Taffe, B. G., and Trush, M. A. Role of free radicals in tumour promotion and progression. *In:* T. J. Slaga, A. J. P. Klein-Szanto, R. K. Boutwell, D. E. Stevenson, H. L. Spitzer, and B. D'Motto (eds.), Skin Carcinogenesis: Mechanisms and Human Relevance, pp. 233–248. New York: Alan R. Liss, Inc., 1989.
7. Wei, H., and Frenkel, K. Suppression of tumor promoter-induced oxidative events and DNA damage *in vivo* by sarcophytol A: a possible mechanism of antipromotion. Cancer Res., *52:* 2298–2303, 1992.
8. Wei, H., and Frenkel, K. *In vivo* formation of oxidized DNA bases in tumor promoter-treated mouse skin. Cancer Res., *51:* 4443–4449, 1991.
9. Wei, H., and Frenkel, K. Relationship of oxidative events and DNA oxidation in SENCAR mice to *in vivo* promoting activity of phorbol ester-type tumor promoters. Carcinogenesis (Lond.), *14:* 1195–1201, 1993.
10. Murakami, A., Ohigashi, H., and Koshimizu, K. Possible anti-tumour promoting properties of traditional Thai food items and some of their active constituents. Asia Pacific J. Clin. Nutr., *3:* 185–191, 1994.
11. Kondo, A., Ohigashi, H., Murakami, A., Jiwajinda, S., and Koshimizu, K. A potent inhibitor of tumor promoter-induced Epstein-Barr virus activation, 1′-acetoxychavicol acetate from *Languas galanga*, a traditional Thai condiment. Biosci. Biotechnol. Biochem., *57:* 1344–1345, 1993.
12. Murakami, A., Nakamura, Y., Koshimizu, K., and Ohigashi, H. Glyceroglycolipids from *Citrus hystrix*, a traditional herb in Thailand, potently inhibits the tumor-promoting activity of 12-*O*-tetradecanoylphorbol-13-acetate in mouse skin. J. Agric. Food Chem., *43:* 2779–2783, 1995.
13. Murakami, A., Ohura, S., Nakamura, Y., Koshimizu, K., and Ohigashi, H. 1′-Acetoxychavicol acetate, a superoxide anion generation inhibitor, potently inhibits tumor promotion by 12-*O*-tetradecanolyphorbol-13-acetate in ICR mouse skin. Oncology, *53:* 386–391, 1996.
14. Nakamura, Y., Murakami, A., Koshimizu, K., and Ohigashi, H. Inhibitory effects of pheophorbide a, a chlorophyll-related compound, on skin tumor promotion in ICR mouse skin. Cancer Lett., *108:* 247–255, 1996.
15. Ohnishi, M., Tanaka, T., Makita, H., Kawamori, T., Mori, H., Satoh, K., Hara, A., Murakami, A., Ohigashi, H., and Koshimizu, K. Chemopreventive effect of a xanthine oxidase inhibitor, 1′-acetoxychavicol acetate, on rat oral carcinogenesis. Jpn. J. Cancer Res., *87:* 349–356, 1996.
16. Tanaka, T., Makita, H., Kawamori, T., Kawabata, K., Mori, H., Murakami, A., Satoh, K., Hara, A., Ohigashi, H., and Koshimizu, K. A xanthine oxidase inhibitor 1′-acetoxychavicol acetate inhibits azoxymethane-induced colonic aberrant crypt foci in rats. Carcinogenesis (Lond.), *18:* 1113–1118, 1997.
17. Tanaka, T., Kawabata, K., Kakumoto, M., Makita, H., Matsunaga, K., Mori, H., Satoh, K., Hara, A., Murakami, A., Ohigashi, H., and Koshimizu, K. Chemoprevention of azoxymethane-induced rat colon carcinogenesis by a xanthine oxidase inhibitor, 1′-acetoxychavicol acetate. Jpn. J. Cancer Res., *88:* 821–830, 1997.
18. Ohigashi, H., Murakami, A., Nakamura, Y., and Koshimizu, K. Anti-tumor promoters from edible Thai plants: isolation, cancer preventive potential, and action mechanisms. *In:* H. Ohigashi, T. Osawa, J. Terao, S. Watanabe, and T. Yoshikawa (eds.), Food Factors for Cancer Prevention, pp. 188–193. Tokyo: Springer-Verlag Tokyo, 1997.
19. Noro, T., Sekiya, T., Katoh, M., Oda, Y., Miyase, T., Kuroyanagi, M., Ueno, A., and Fukushima, S. Inhibitors of xanthine oxidase from *Alpinia galanga*. Chem. Pharm. Bull., *36:* 244–248, 1988.
20. Collins, S. J., Gallo, R. C., and Gallagher, R. E. Continuous growth and differentiation of human myeloid leukaemic cells in suspension culture. Nature (Lond.), *270:* 347–349, 1977.
21. Wei, H., Wei, L., Frenkel, K., Bowen, R., and Barnes, S. Inhibition of tumour promoter-induced hydrogen peroxide formation *in vitro* and *in vivo* by genistein. Nutr. Cancer, *20:* 1–12, 1993.
22. Markert, M., Andrews, P. C., and Babior, B. M. Measurement of O_2^- production by human neutrophils. The preparation and assay of NADPH oxidase-containing particles from human neutrophils. Methods Enzymol., *105:* 358–365, 1984.
23. Nakamura, Y., Ohto, Y., Murakami, A., Osawa, T., and Ohigashi, H. Inhibitory effects of curcumin and tetrahydrocurcuminoids on the tumor promoter-induced reactive oxygen species generation in leukocytes *in vitro* and *in vivo*. Jpn. J. Cancer Res., *89:* 361–370, 1998.
24. Bass, D. A., Parce, J. W., Dechatelet, L. R., Szejda, P., Seeds, M. C., and Thomas, M. Flow cytometric studies of oxidative product formation by neutrophils: a graded response to membrane stimulation. J. Immunol., *130:* 1910–1917, 1983.
25. Reiners, J. J., Jr., Pence, B. C., Barcus, M. C. S., and Cantu, A. R. 12-*O*-Tetradecanoylphorbol-13-acetate-dependent induction of xanthine dehydrogenase and conversion to xanthine oxidase in murine epidermis. Cancer Res., *47:* 1775–1779, 1987.
26. Takeuchi, T., Nakajima, M., and Morimoto, K. Relationship between the intracellular reactive oxygen species and the induction of oxidative DNA damage in human neutrophil-like cells. Carcinogenesis (Lond.), *17:* 1543–1548, 1996.
27. Lundqvist, H., Follin, P., Khalfan, L., and Dahlgren, C. Phorbol myristate acetate-induced NADPH oxidase activity in human neutrophils: only half the story has been told. J. Leukocyte Biol., *59:* 270–279, 1996.
28. Yamamoto, S., Kiyoto, I., Aizu, E., Nakadate, T., Hosoda, Y., and Kato, R. Differential inhibition by staurosporine, a potent protein kinase C inhibitor, of 12-*O*-tetradecanoylphorbol-13-acetate-caused skin tumor promotion, epidermal ornithine decarboxylase induction, hyperplasia and inflammation. Carcinogenesis (Lond.), *10:* 1315–1322, 1989.
29. Watanabe, N., Kataika, T., Tajika, T., Uramoto, M., Magae, J., and Nagai, K. 1′-Acetoxychavicol acetate as an inhibitor of phagocytosis macrophages. Biosci. Biotechnol. Biochem., *59:* 1566–1567, 1995.
30. Nakae, D., Mizumoto, Y., Yoshiji, H., Andoh, N., Horiguchi, K., Shiraiwa, K., Kobayashi, E., Endoh, T., Shimoji, N., Tamura, K., Tsujiuchi, T., Denda, A., and Konishi, Y. Different roles of 8-hydroxyguanine formation and 2-thiobarbituric acid-reacting substance generation in the early phase of liver carcinogenesis induced by a choline-deficient, L-amino acid-defined diet in rats. Jpn. J. Cancer Res., *85:* 499–505, 1994.
30. Farber, E. Cellular biochemistry of the stepwise development of cancer with chemicals: GHA Clowes Memorial Lecture. Cancer Res., *44:* 5463–5474, 1984.
31. Petruska, J. M., Mosebrook, D. R., Jakab, G. J., and Trush, M. A. Myeloperoxidase-enhanced formation of (±)-*trans*-7,8-dihydroxy-7,8-dihydrobenzo[*a*]pyrene-DNA adducts in lung tissue *in vitro*: a role of pulmonary inflammation in the bioactivation of a procarcinogen. Carcinogenesis (Lond.), *13:* 1075–1081, 1992.
32. Trush, M. A., Egner, P. A., and Kensler, T. W. Myeloperoxidase as a biomarker of skin irritation and inflammation. Food Chem. Toxicol., *32:* 143–147, 1994.
33. Warren, J. S., Yabroff, K. R., Mandel, D. M., Johnson, K. J., and Ward, P. A. Role of O_2^- in neutrophil recruitment into sites of dermal and pulmonary vasculitis. Free Radical Biol. Med., *8:* 163–172, 1990.
34. Thomas, D. W., Matthews, J. B., Patel, V., Game, S. M., and Prime, S. S. Inflammatory cell infiltrate associated with primary and transplanted tumours in an inbred model of oral carcinogenesis. J. Oral Pathol. Med., *24:* 23–31, 1995.
35. Grisham, M. B., Ware, K., Gilleland, H. E., Jr., Gilleland, L. B., Abell, C. L., and Yamada, T. Neutrophil-mediated nitrosamine formation: role of nitric oxide in rats. Gastroenterology, *103:* 1260–1266, 1992.